Characterizing pathology in erythrocytes using morphological and biophysical membrane properties: relation to impaired hemorheology and cardiovascular function in rheumatoid arthritis

Oore-ofe O Olumuyiwa-Akeredolu[1], Prashilla Soma[2], Antoinette V Buys[3], Legesse Kassa Debusho[4], Etheresia Pretorius[5,*]

[1]Department of Physiology, Faculty of Health Sciences, University of Pretoria, Private Bag X323, Arcadia, 0007, RSA. Oore.Olumuyiwa@up.ac.za

[2]Department of Physiology, Faculty of Health Sciences, University of Pretoria, Private Bag X323, Arcadia, 0007, RSA. Prashilla.Soma@up.ac.za

[3]Unit for Microscopy and Microanalysis, Department of Anatomy and Physiology, Faculty of Veterinary Sciences, University of Pretoria. Antoinette.Buys@up.ac.za

[4]Department of Statistics, University of South Africa, Pretoria RSA. Debuslk@unisa.ac.za

[5]Department of Physiological Sciences, Stellenbosch University, Private Bag X1, Matieland, 7602, RSA. Resiap@sun.ac.za

***Corresponding Author:**

Etheresia Pretorius
Department of Physiological Sciences
Faculty of Natural Sciences
Stellenbosch University
Stellenbosch
South Africa
Phone: 27 829295041
Fax: 27 21 808 3145
E-mail: resiap@sun.ac.za

Highlights

- Erythrocytes (RBCs) in rheumatoid arthritis (RA) have reduced elasticity.
- RBCs in RA display a wide range of poikilocytosis.
- RBCs in RA display membrane pathomorphology.
- Band 3 skeletal protein network is altered in RA RBCs.
- Specific poikilocytes have been identified frequently with the use of NSAIDs or the presence of cardiovascular comorbidities.

Authorship/Acknowledgments

OOA performed the research study, analysed and interpreted its outcomes and wrote this paper. PS was the physician who screened, selected, and drew blood from all study participants. LKD was the statistician who performed analyses for data obtained from AFM studies. EP designed and appraised the study and its outcomes. AVB performed collation of the AFM data. Assistance with utility of microscopes was provided by staff of the Laboratory for Microscopy and Microanalysis, University of Pretoria. All authors read and approved the manuscript.

Funding

Medical Research Council: E Pretorius (fund number A0X331) and National Research Foundation: E Pretorius (fund number: N00345).

Graphical abstract

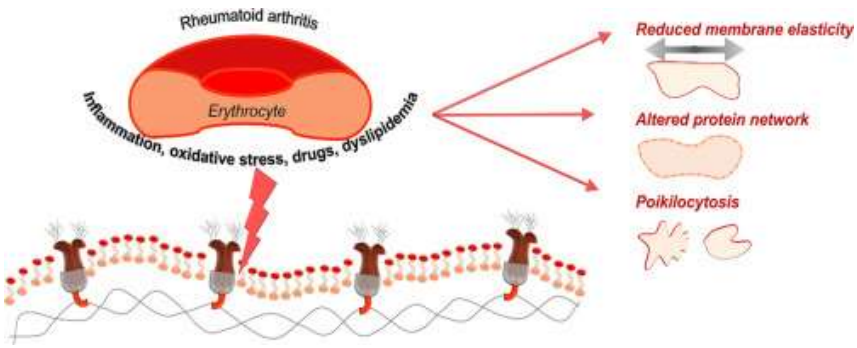

Abstract

The inflammatory burden of the complex Rheumatoid Arthritis (RA) disease affects several organ-systems, including rheological properties of blood and its formed elements. Red blood cells (RBCs) are constantly exposed to circulating dysregulated inflammatory molecules that are co-transported within the vasculature; and their membranes may be particularly vulnerable to the accompanying oxidative stress. In the current study, we investigate biophysical and ultrastructural characteristics of RBCs obtained from a cohort of patients using atomic force microscopy (AFM), scanning electron microscopy (SEM) and confocal microscopy (CM). Statistical analyses of AFM data showed that RA RBCs possessed significantly reduced membrane elasticity relative to that of RBCs from healthy individuals (P-value < 0.0001). SEM imaging of RA RBCs revealed increased anisocytes and poikilocytes. Poikilocytes included knizocytes, stomatocytes, dacryocytes, irregularly contracted cells, and knot cells. CM imaging of several RA RBCs, spectrin, and band 3 protein

networks portrayed the similar morphological profiles. Analyses of CM images confirmed changes to distribution of band-3 skeletal protein, a protein critical for gaseous exchange functions of the RBC and preventing membrane surface loss. Decreased membrane deformability impairs the RBC's capacity to adequately adapt its shape to navigate blood vessels, especially microvasculature, and this decrease is also reflected in the cell's morphology. Changes to morphology and deformability may also indicate loss of functional domains and/or pathological protein and lipid associations. These findings suggest that RA disease and/or its concomitant factors impact on the RBC and its membrane integrity with potential for exacerbating pathological cellular function, hemorheology, and cardiovascular function.

Keywords

Rheumatoid arthritis, erythrocyte, membrane, poikilocytes, atomic force microscopy, rheology.

1. INTRODUCTION

Rheumatoid arthritis (RA) is an inflammatory autoimmune disease with complex aetiology and pathobiology and varied manifestations across affected individuals although a common pathological feature is changed blood rheology, frequently manifesting as raised RBC sedimentation rates. The inflammatory burden of RA affects several organ-systems in addition to its articular influences. The circulatory system and its cells are suspected to be less-detected extraarticular targets of the disease and its inflammatory mediators, such as IL-6, which has been demonstrated to change the morphological features of healthy blood (1, 2). There is ample evidence that RA-induced inflammation inflicts oxidative assault on the RBC and affects its biochemical and physiological activities within circulation (3-7). Free radicals in blood reduce protective membrane thiols and antioxidant enzymes like

superoxide dismutase while generating dysfunction in the ion transport ATPases of RA RBCs (8). Rheology and hemodynamics of blood are compounded by morphopathological changes to the RBC membrane (9). Capacity for gaseous exchange functions of integral proteins and overall skeletal integrity may also be compromised by membrane damage (10, 11).

RBC-associated indices correlate with some markers of inflammation in RA. Among those reported are RBC sedimentation rate (ESR), haemoglobin levels, and RBC counts, which were found to correlate with levels of radiographic erosion (12, 13). Elevated fibrinogen concentration and IgG levels in RA patients have been shown to correlate with increased plasma viscosity (14). Increased ESR and fibrinogen levels are also hemorheologic markers and indicators of RA disease progression (15). These markers implicate the autonomous contribution of RBCs morphopathology, besides other factors in plasma, to hemorheological disorders in RA.

Of late, the Center for Disease Control and Prevention reported an ongoing rise in arthritis prevalence in the United States adult population, amongst which RA is included (16). Cardiovascular (CV) diseases have been demonstrated to be a significant source of mortality in affected persons. In 2016, the European League Against Rheumatism taskforce made recommendations for expert opinion-based screening for CV risk factors (17). Besides vascular and cardiac tissue integrity, blood and especially the RBC, is critical to performing this critical assignment of CV risk assessment considering it makes up over 90% of formed elements within blood. In cardiovascular diseases, RBC indices have been implicated in impaired blood rheology. A direct relationship has been found between decreased RBC deformability and increased risk for arterial hypertension in non-RA conditions (18). RBC distribution width (RDW) values above a 14% threshold were associated with

decreased cellular deformability (19). A parallel association was also found between RDW and the occurrence of acute myocardial infarction in RA patients excluding individuals with other cardiovascular diseases (20). Under conditions of increased shear stress, as typically occur in microvasculature, RBCs' deformability determine efficacy of tissue perfusion, but even shape and surface attributes determine optimized blood flow rate in larger vessels (9).

As discussed, the RBC's biophysical properties are critical to blood rheology, RA pathophysiology, and the occurrence of cardiovascular comorbidities. Subsequently, we discuss its structure and function.

1.1 Erythrocyte Membrane Structure

The RBC membrane comprises a phospholipid bilayer, an underlying supporting skeleton, integral, transmembrane, and anchoring biomolecules. Two key components of underlying skeleton, which are critical to and indicative of the integrity of the cell's structure, are the band 3 integral membrane protein and the cytoskeletal spectrin network. Anion exchanger 1 or band 3 is an important biomolecular switch that mediates oxygen-regulation of the cell's functions such as the assembly of crucial metabolic enzymes, interaction of ankyrin with band 3, and ATP release (21). A hexagonal spectrin lattice comprising interwoven α and β chains is anchored by ankyrin to a complex made up of band 3, CD47, protein 4.2 (pallidin) and Rh proteins, which all contribute to the cell's structural integrity (10, 22, 23). Other membranous biomolecular inclusions are flippase, floppase, and scramblase which control the transfer of phospholipids from inner to outer leaflets, lipid rafts comprising stomatin, tightly packed outer leaflet sphingolipids, the glycosylphosphatidylinositol-bound enzyme acetylcholinesterase, inner leaflet phosphatidylserine and

phosphatidylethanolamine with which flotillin non-covalently associates while cholesterol interacts with hydrophobic tails (24). Cholesterol is embedded between the membrane leaflets, and its augmentation within this space results in decreased cellular permeability and fluidity (25, 26). There are also inorganic molecule transporters such as: glut 1 anchored to the actin-tropomyosin-tropomodulin complex by dematin and adducin, glycophorin anchored by protein p55 to protein 4.1 and the spectrin network, calcium pumps, and aquaporins (24).

A pathological coagulation system, including damage to RBCs, are hallmarks of systemic inflammation, that are known to be present in RA. Systemic inflammation in RA may lead to a reduction in the RBC's biomechanical and viscoelastic capacity. The RBC's deformability and fluidity influenced by cell volume and membrane structure are critical determinants of its capacity to navigate smaller vasculature like capillaries. Given that inflammatory cytokines like IL-6, a key regulator in RA pathobiology (27), have been demonstrated to result in pathological changes in RBCs within whole blood (2), here we investigate biophysical properties of RBCs obtained from patients affected by RA.

2. MATERIALS AND METHODS

2.1 Ethics

Ethical approval for this study was obtained from the Human Ethics Committee of the University of Pretoria's Faculty of Health Sciences on the 20th of November 2013 (Ethical clearance number 462/2013). All participants signed informed consent forms with participant information held and utilized anonymously and confidentially. Research protocols were performed in adherence to requirements stipulated in the Declaration of Helsinki.

2.2 Sample

2.2.1 Patient group

Thirty-nine RA patients, screened and diagnosed using the 2010 RA classification criteria of the American College of Rheumatology (ACR), of both genders and over the age of 18 were chosen for this study. Selected participants were diagnosed at least 6 months prior to the study's commencement with the disease managed using analgesics and non-biologic antirheumatics prior to blood collection. Volunteers were recruited from the Steve Biko Academic Hospital's Department of Internal Medicine, Rheumatology Unit in Pretoria.

2.2.2 Control group

Thirty healthy control subjects of both genders and above 18 years of age were selected for this study. Control participants were volunteers recruited from within the Pretoria locality.

2.3 Exclusion criteria

Exclusion criteria for the RA study group were individuals who were pregnant or lactating, diagnosed with or suffering from hepatic, or kidney disease.

Exclusion criteria for the control group were smokers, subjects with cardiovascular diseases, clotting disorders, or other inflammatory disorders. Individuals who were pregnant, lactating, undergoing hormonal therapy, or using anticoagulants of any kind were also excluded from control group.

2.4 Blood collection

A qualified physician collected blood once from patient and control subjects in citrate tubes containing 0.5mls of 3.8% sodium citrate. The blood was left to combine with anticoagulant for 30 minutes prior to further preparation.

2.5 Atomic Force Microscopy Technique

1µL aliquots of the whole blood samples obtained in microtubes were centrifuged at 7.5rpm for 30 seconds and the plasma supernatant was discarded. The pelleted RBC fraction was retrieved and resuspended in a 0.0375M sodium phosphate buffer solution (PBS). 2.5% glutaraldehyde and 1% osmium tetroxide were used as primary and secondary fixation agents, respectively. Between fixation steps, samples were washed in the PBS buffer, followed by dehydration using a graded series of ethanol. Finally, samples were optimized for uniform drying by immersion in hexamethyldisilazane (HMDS) for 30 minutes. Then, a 5µL suspension of cells was pipetted and dropped onto glass slides adapted for use with the atomic force microscope.

AFM analysis was carried out using Dimension Icon, system manufactured by Bruker, USA operated in Peak Force Quantitative Nanomechanical Mapping (QNM) mode. This mode operates by applying a controlled force at each data point, resulting in a quantitative force distance curve from which the Young's Modulus (YM) can be determined using the slope of the retract curve. YM is a measure of elasticity, or the ability of a material to return to its original shape after having been deformed by a fixed amount of force; higher YM values indicate decreased elasticity.

This is achieved by fitting the slope of the retract curve with the Derjaguin–Muller–Toporov (DMT) model (28): $F - F_{adh} = 4/3\ E^* \sqrt{R}\ (d - d_o)^3$, where $F - F_{adh}$ is the force

on the cantilever relative to the adhesion force, R is the tip end radius, ($d - d_o$) is the deformation of the sample and E^* is the reduced modulus. If Poisson's ratio is known, the YM can be calculated according to $E^* = [(1 - v_s^2) / E_s + (1 - v_{tip}^2) / E_{tip}]^{-1}$, where v_s is the Poisson's ratio of the sample (for cells 0.5 is established; perfectly incompressible), v_{tip} is the Poisson's ratio for the probe. E_s and E_{tip} are the YM of the sample and the probe respectively.

Silicon Nitride probes (TAP525-MPP13120, Bruker USA) with a nominal spring constant of 200 $N.m^{-1}$, a resonant frequency between 430 and 516kHz and a nominal tip radius of 15nm were used to evaluate membrane elasticity. A randomly selected scan area of 1µm on the convex surface of each RBC was chosen for assessment. 30 cells from each participant/patient were analysed at a scan rate of 0.6 hertz. Approximately 50 force curves were then randomly selected from the area and fit to the DMT model using Nanoscope Analysis software (Bruker, USA). Approximately 1500 data points was therefore collected for each participant/patient RBC, only force curves with a goodness of fit of 0.85 and above was used for statistical analysis. Analysis was performed in cool ambient air at 30% relative humidity at a scan rate of 0.6 hertz.

2.5.1 Statistics

Statistical analysis was done using the free statistical package R, Version 3.3.0 for windows (29). Calculations of standard deviation were done using the formula: $SD_{\bar{x}} = \sum (x - \bar{x})^2 / (n - 1)$, while standard error was calculated using: $SE_{\bar{x}} = SD_{\bar{x}} / \sqrt{n}$.

2.6 Scanning Electron Microscopy Technique

RBCs in blood samples that had been smeared, and fixed on small glass slides for SEM studies following methods previously described (30) were examined in RA and control subjects. Each was mounted on aluminium plates adapted for use in the microscope, and carbon coated to enable conduction and SEM imaging.

A Zeiss ULTRA plus FEG-SEM with InLens capabilities was used to study the surface morphology of RBCs and all micrographs were taken at 1kV.

2.7 Confocal Microscopy Technique

An RBC fraction was obtained from each fractionated blood sample and 20µL acquired for staining. 1ml of fixative (3% formaldehyde) was added to each sample and incubated for 5 minutes at 20-25^{o}C. The fixed sample was then washed 3 times with PBS for 3 minutes each. A 2% solution of primary antibodies (ab11012 and ab11751, Abcam) was added to each sample and this was incubated for a minimum of 90 minutes or maximally overnight and then washed twice. A 2% solution of secondary antibodies (ab97244 and ab130785, Abcam), which had been coupled with the fluorophores fluorescein isothiocyanate (FITC) and allophycocyanin/cyanine 7 (APC/Cy7) respectively was added to each sample and the solution was incubated at room temperature in the dark for 60 minutes. Details on antibodies employed in the study of skeletal membrane protein structure are summarized in table 2. Each sample was washed twice and re-suspended in 5µL of fresh buffer. 1µL of the sample was then mounted onto glass slides adapted for use with the microscope.

Samples were viewed using a Zeiss Laser Scanning Microscope (LSM) 510 META confocal microscope with a Plan-Apochromat 63x/1.4 Oil DIC objective. The

following filters were used: Ch3: BP 505-550 and ChS1: 636-754 with wavelengths of 488 nm and 633 nm.

2.7.1 Analyses of Confocal Image Data

Analyses of the RBC indices in acquired micrographs were performed using the shape descriptors function in ImageJ (31). Values obtained were acquired using the following calculations:

A. Circularity

$$Circularity = 4\pi \times [Area] / [Perimeter]^2$$

with a value of 1.0 indicating a perfect circle. As the value approaches 0.0, it indicates an increasingly elongated shape.

B. Aspect ratio of the particle's fitted ellipse

$$Aspect\ ratio = [Major\ Axis] / [Minor\ Axis]$$

C. Roundness

$$Roundness = 4 \times [Area]\pi \times [Major\ axis]^2$$

or the inverse of its Aspect Ratio.

D. Solidity

$$Solidity = [Area] / [Convex\ area]$$

The calculated values for each of the four parameters were evaluated using box-and-whisker plots.

In a recent article, we emphasized the usefulness of employing RBC structure as an index of inflammatory activity in the application of individualized precision medicine

(24). Here, we present evidence of differences existing in membrane structure of RBCs obtained from RA patients when compared to healthy individuals.

3. RESULTS

3.3.1 Atomic Force Microscopy Findings on Erythrocyte Membrane Elasticity

12, 877 YM values of RBCs obtained from 13 healthy individuals and 24, 392 values from 30 patients were analysed. A significant difference was found between the mean apparent elastic modulus (AEM) values obtained for RBCs from RA patients (55,003 AEM) and controls (44,644 AEM) illustrating a 23% increase. A one-way analysis of variance (ANOVA) comparison of YM values between RA patient and healthy control RBCs demonstrated significantly higher YM values for RBC membrane surfaces assessed from the RA group when compared to those assessed from the healthy control group (p-value < 0.0001). Table 1 provides a summary of the results from statistical analyses.

Table 1: Descriptive statistics on apparent elastic modulus (AEM) of RBC membranes obtained using atomic force microscopy

	Controls	**RA**
Mean AEM	44,644	55,003
Standard error	382	283
Standard deviation	43,378	44,251
Significance compared to control (P-value)	-	1.0892e-13
N (cells)	480	960
N (curves)	12877	24392

Force distance curves were generated by plotting the force required by the cantilever to generate a displacement on the RBC membrane. The angle formed by the contact region slope of the retraction curve (DMT model) is used to calculate the YM values. A steeper curve as detected with curves from RA RBCs, generates greater YM values. The resulting graph is illustrated in Figure 1.

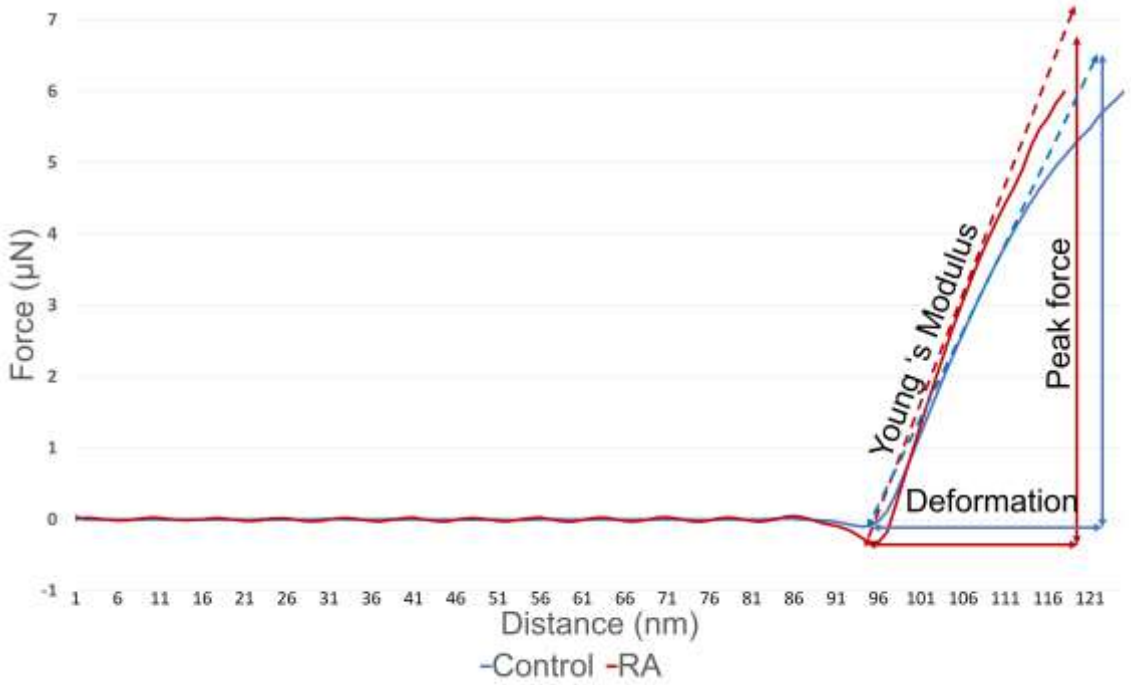

Figure 1: Force-distance curves representing average force measurements obtained for RBCs from rheumatoid arthritis (RA) and control individuals. The force-distance curves illustrate the range of the cantilever's deflection on the RBC surface.

3.3.2 RBC Membrane Morphology and Skeletal Protein Network

Figure 2 shows SEM images illustrating a healthy control RBC and representative normocytes (size 6.2 to 8.2µm) identified within the RA group. Figure 3 follows with analogous confocal imaging of skeletal framework. Spectrin and band-3 proteins, which contribute significantly to structural integrity of the cell, were fluorescently tagged red and green respectively.

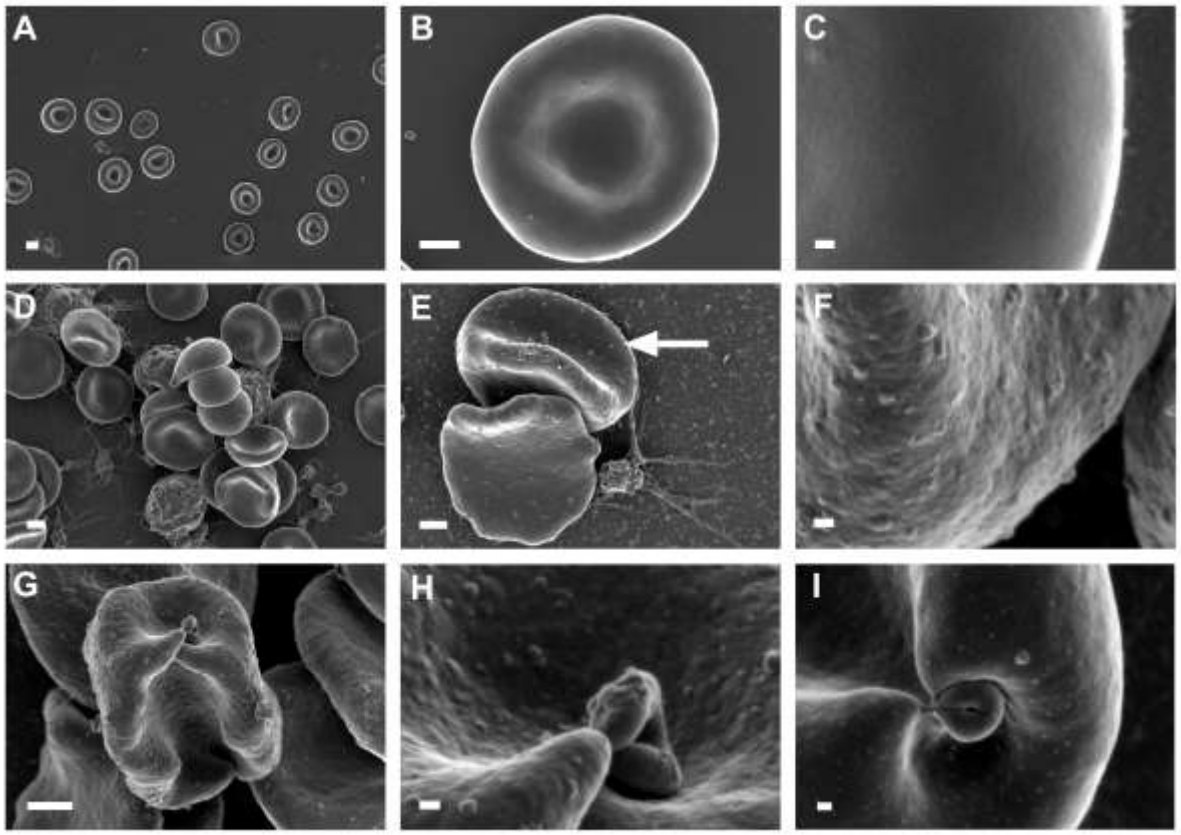

Figure 2: SEM micrographs of RBCs in whole blood smears. 'A': overview of RBCs from control group; 'B': single RBC from control group; 'C': machine-magnification of control RBC membrane in 'B'; 'D': overview of an aggregate of RBCs (stomatocytes stacked in center), leukocytes, and platelets in RA whole blood; 'E': close view of 2 RA RBCs - white arrow indicates knizocyte and the other is a leptocyte; 'F': machine-magnification of a knizocyte membrane from RA whole blood; 'G': an RBC with knotted membrane; 'H': machine-magnification of knot in 'G'; 'I': machine magnification of a knot in another RBC from RA whole blood. Scale in 'A' and 'D': 2μm; scale in 'B', 'E', and 'G': 1μm; scale in 'C', 'F', 'H', and 'I': 100nm.

The band 3 transmembrane protein is integrated within the lipid bilayer while the spectrin network is closely bound to the inner leaflet. We employed the fluorescent-coupled antibodies earlier described to map the configuration of the protein network formed by spectrin and band 3 within the RBC membrane. By fluorescently tagging these two proteins, we illuminate the 3-dimensional structure of the RBC membrane. The confocal micrographs represent a cross-sectional segment within a 3-dimensional skeletal framework. Efforts were made to select images that captured the most central cross-section of each cell outline, often at the widest radius.

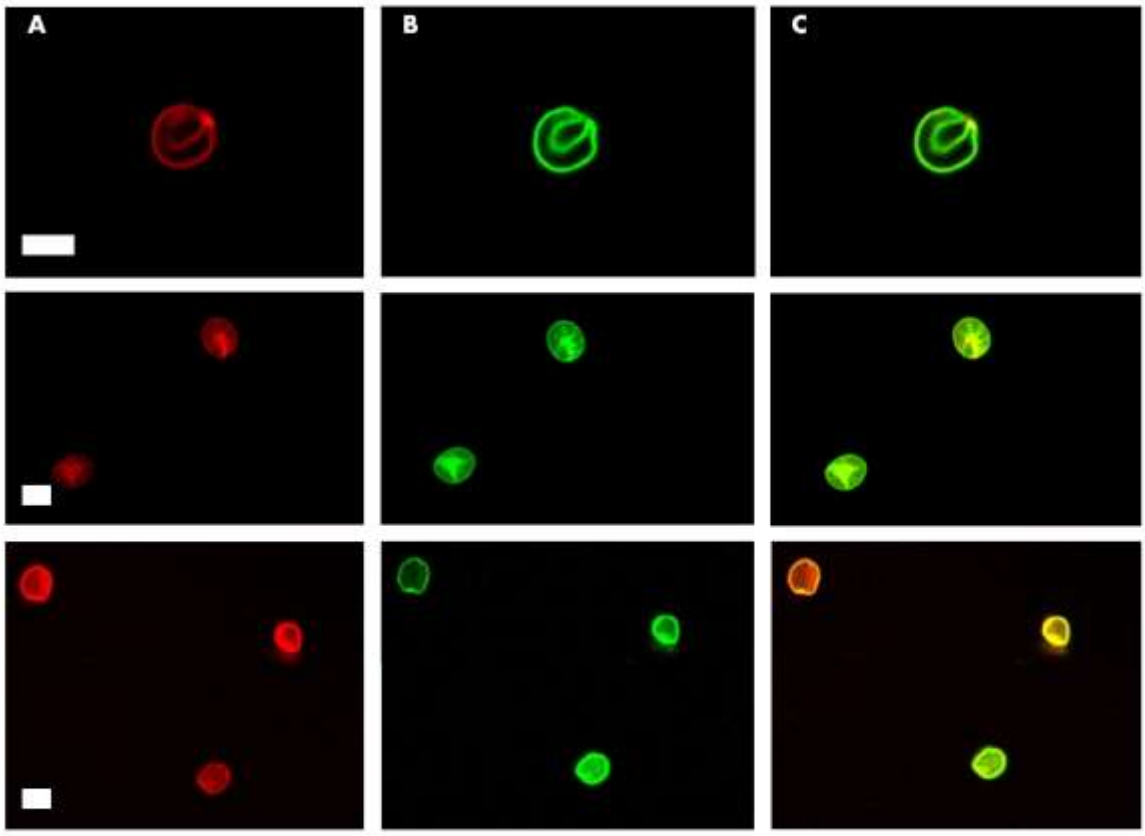

Figure 3: CM images of some control RBCs showing underlying skeletal proteins outlining discocyte or normocyte shapes (circular outline). 'A' (red): spectrin network, 'B' (green): band 3 network, 'C': superimposed imaging of both protein networks. Scale: 5µm

In several RA patients, some RBCs shapes and sizes varied from the discocyte. Examples of poikilocytes and anisocytes we frequently detected were knizocytes, stomatocytes, acanthocytes, and microcytes or irregularly contracted cells. Some of these are illustrated in figure 4.

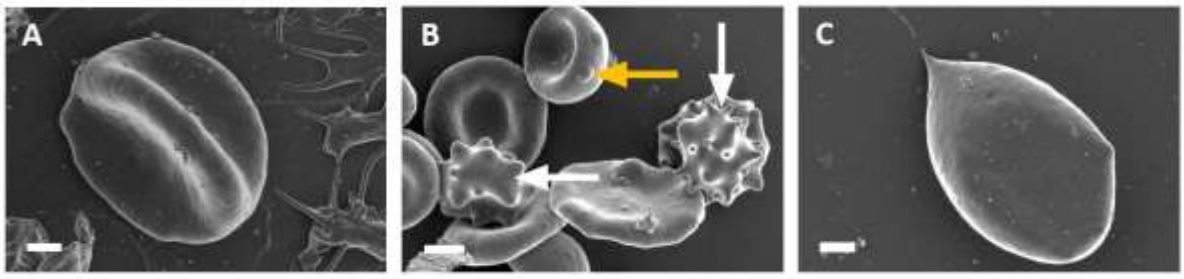

Figure 4: SEM micrographs of some identified RA anisopoikilocytes: 'A': knizocyte, 'B': stomatocyte showing membrane blistering (yellow arrow), and acanthocytes (white arrows), 'C': irregularly contracted cell. Scale in 'A' and 'C': 1µm; scale in 'B': 2µm.

Figure 5 follows with congruent confocal images of RA RBCs showing spectrin and band 3 protein networks that show the outline of knizocytes.

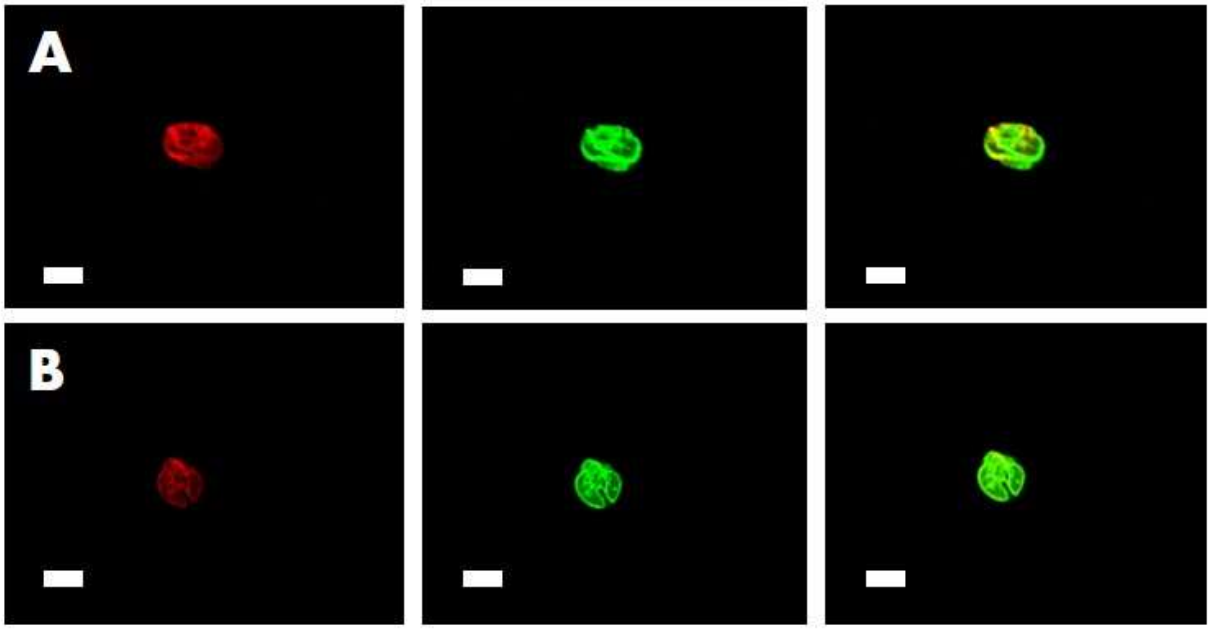

Figure 5: CM images of two RA RBCs showing skeletal network of spectrin (red) and band 3 (green) proteins followed by a superimposition of labels on both proteins. 'A': skeletal network of these proteins takes on the contour of an inverted knizocyte & 'B': a superior view of the protein network outlines the characteristically pinched shape of a knizocyte. Scale: 5µm

The arrangement of band 3 ion exchange proteins central to maintenance of RBC membrane integrity was investigated. Averages of composite dimensions of RBC cross-sections acquired from CM images of the band 3 network in controls and RA

RBCs were compared using ImageJ shape descriptors. Table 2 shows a summary of the analyses.

Table 2: Statistical summary of dimensional analyses made on band 3 network on outer leaflet reported as mean (± standard error of mean)

		Average of measurements			
	N cells	**Circularity**	**Aspect ratio**	**Roundness**	**Solidity**
Control	100	0.950 (±0.005)	1.150 (±0.012)	0.878 (±0.008)	0.988 (±0.002)
RA	150	0.858 (±0.008)	1.320 (±0.020)	0.782 (±0.011)	0.965 (±0.003)

Figure 6 displays charts showing the distribution of values obtained for measured dimensions of the band 3 membrane protein in control and RA RBC groups.

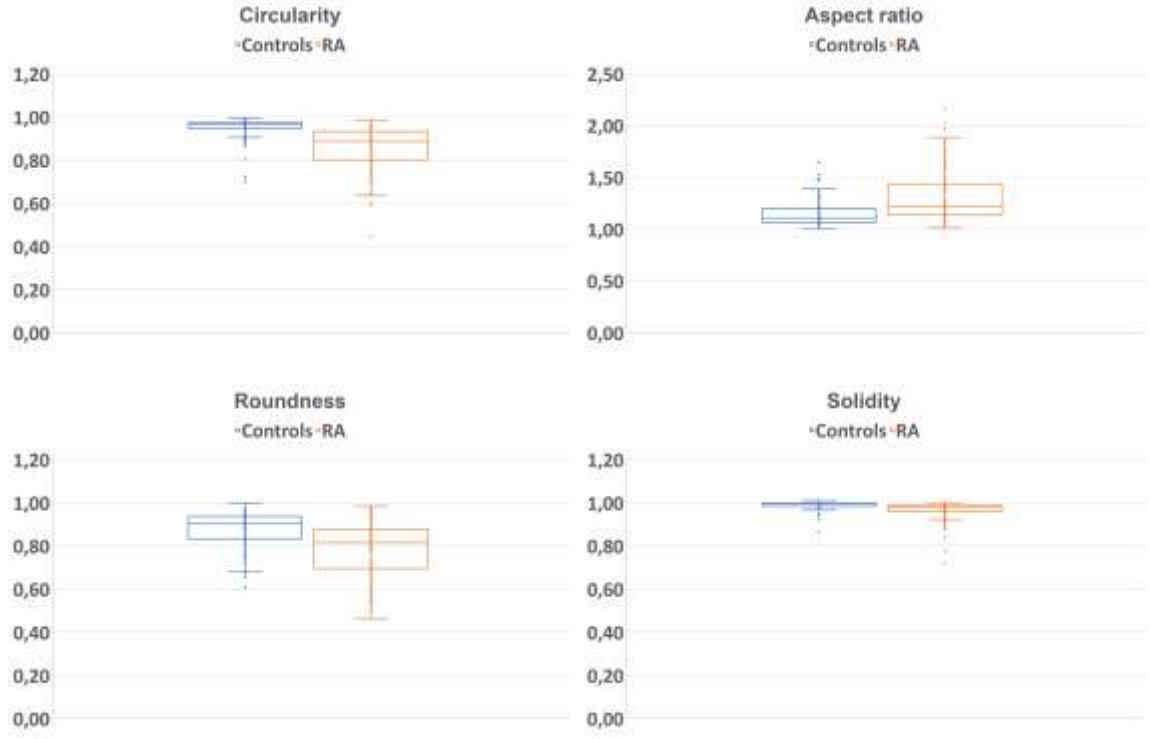

Figure 6: Box-and-whisker plot representation of four morphological parameters of band 3 protein network in membranes of control and RA RBCs. Circularity, roundness, aspect (axial) ratio and solidity parameters of outlines formed by the protein within the membrane were measured from confocal images of 100 control RBCs and 150 RA RBCs.

RA RBCs had a protein distribution displaying relatively lower circularity, roundness, and solidity but increased aspect ratio values than the control group. 86.7% of cells in the RA group had a protein network with lower circularity values than the mean of the control group. 80% of RBCs in the RA group had increased aspect ratio while 74% had reduced roundness than the mean of the control group. Finally, 80% of RBCs in the RA group had reduced solidity compared to the mean of the control group.

Other poikilocytes identified among RA RBCs are illustrated in figure 7. Among these are microcytes, stomatocytes, elliptocytes, and irregularly contracted cells.

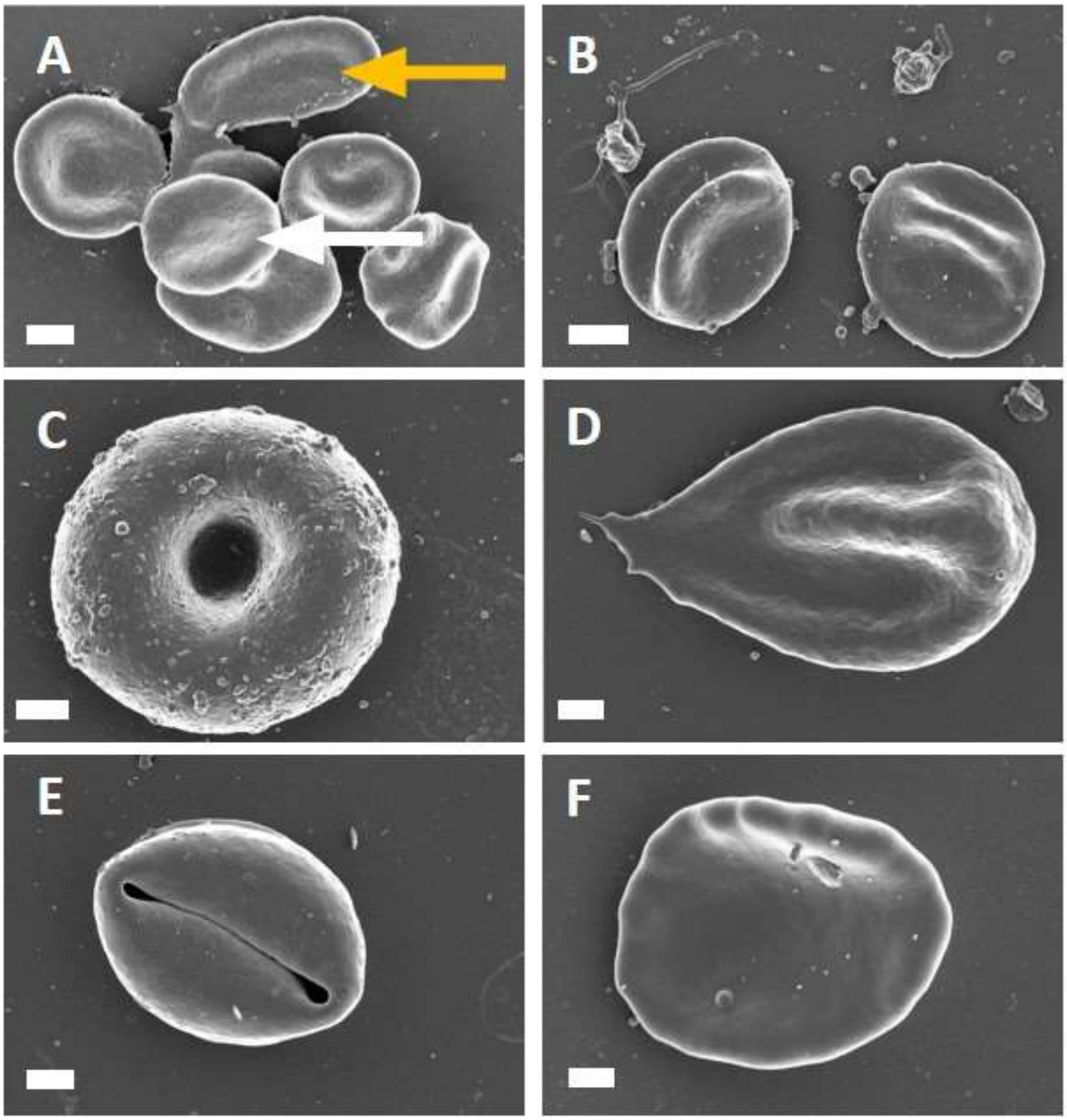

Figure 7: SEM micrographs of commonly identified RA anisopoikilocytes: 'A': group of RBCs including an elliptocyte (yellow arrow) and a microcyte (white arrow), 'B': two knizocytes with adjacent platelets, 'C': spherocyte with membrane-bound vesicles, 'D': knizodacryocyte, 'E': another stomatocyte, 'F': leptocyte. Scale: 1µm.

Several poikilocytes, which were captured via CM imaging of RA RBCs show cross-sectional outlines of band-3 proteins, and are also non-supportive of the discocyte structure. These are displayed in figure 8.

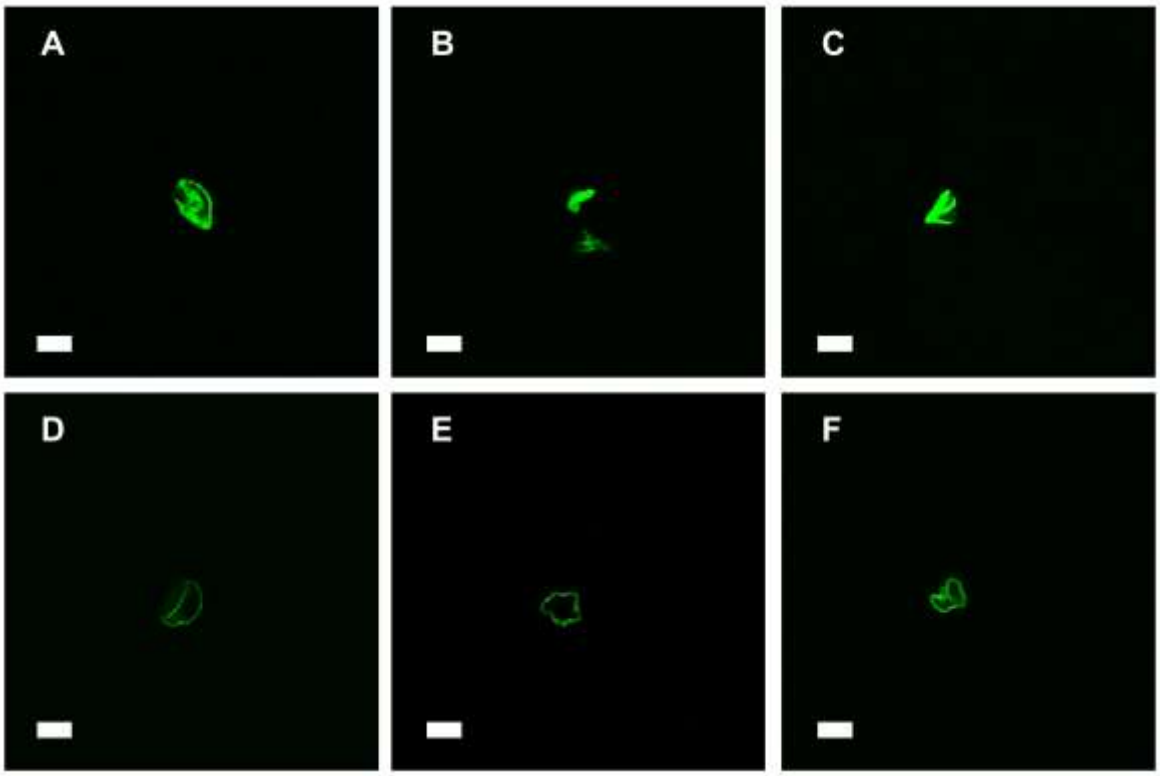

Figure 8: CM images showing the band 3 skeletal protein network on outer leaflet in RBCs from different RA patients. ‘A’, and ‘C’: Non-circular protein networks, ‘D’: side view of a codocyte, ‘B’, ‘E’ and ‘F’: irregularly contracted cells. Scale: 5µm

Table 3 follows below with a summary of morphopathological changes identified via SEM and CM studies of RBCs with associated comorbid conditions and anti-inflammatory drug use in RA subjects.

Table 3: Summary of patient data and associated poikilocytes detected.

Age	Comorbidities	NS	Kni	St	Dac	Sph	Lep	Knot	Irc	Ac/Ec	M/m	El
72	HBP	Y	+	+								
54*	HBP, HCh	Y										
59*	HT	N										
57	HBP, GERD	Y		+		+						
62	HT, As, GERD	Y	+	+								
53	HT, GERD	Y	+++	+++		+		+				
62	HT, DB, GERD	N		+++								
73	HBP, Hyth	N		++	+	+					+	+
62	HCh, Hyth	Y	+	+								
67	HCh, GERD	Y	+	+++		+				+		
54	HT, HBP, GERD	Y	+++	+	+++							
56	HT, HBP, GERD	Y	++	+		+						
60	HT, DB, GERD	Y	+	+								+
59	HT, HBP, GERD	Y			+					+		
44	As, LBP, GERD	Y	+	++			+					
81	HBP, Hyth	Y		++	+			+	+++			++
59	HT, HBP, GERD	N		++								
62	HT, GERD	Y	+	+	+				+++			
67	HBP	Y	+	++								
27	LBP	N		++				+	++			
59	Unk	Unk		++								

54	HT, An, GERD	N		++		+						
53	HT	Y		+			+		++	+		
60	HT, HCh, GERD	Y	++	+++				+				
68	HBP, GERD	Y	++		+++							
49	HT, HBP	Y	++	++								
61	HBP, Dep, GERD	N	+	+++								
37	HCh, Dep, GERD	Y	+	+								
61	HT, Dysl, Hyth, GERD	Y	+	+++	+							
48	HT	Y		++			++					
47	HT, HCh, GERD	Y	+	+++					+			
33	PE	Y	+	+++	+			+	+			
58	GERD	N		+++		+		+				
33	HBP, GERD	Y	+	++		+		+				
53	GERD	Y	+									
34	HT, GERD	Y	+	++								
59	None	Y		++		+		+				
83	Unk	Unk		+++						+		
41	Unk	Unk	++				+++			++		

Ac/Ec = acanthocyte/echinocyte, Comor = comorbidity, Dac = dacryocyte, Dep = depression, Dysl = dyslipidemia, El = elliptocyte, GERD = gestrointestinal reflux disease, HBP = high blood pressure, HCh = high cholesterol, HT = hypertension, Hyth = hypothyroidism or thyroid dysfunction, Irc = irregularly contracted cell, Kni = knizocyte, Knot = knot cell, Lep = leptocyte, LBP = low blood pressure, M/m = macrocyte/microcyte, NS = non-steroidal inflammatory drug use, PE = pulmonary embolism, Sph = spherocyte, St = stomatocyte, Unk = unknown, * = dense matted (plasma) deposits made RBCs hard to detect, + = mildly detected (5-10%), ++ = moderately detected (10-15%), +++ = large numbers (severe comprising over 15% of detected cells).

Data as indicated in the table demonstrates the prominence of stomatocytes in 85% of all the RA subjects, while it was detected in 90% of the subjects who had a previously reported cardiovascular event. Knizocytes were distinguished in 75% of the patients known to be using non-steroidal anti-inflammatory drugs (NSAIDs) and one patient who was not reported to be on any. Dacryocytes were detected in 20% of the patients but did not correlate with record of any specific comorbidity as with other identified poikilocytes. Irregularly contracted cells were common to individuals with cardiovascular dysfunction including hypertension, high blood pressure and even low blood pressure. The occurrence of ovalocytes or pencil cells was common to only two patients with hypothyroidism and one with diabetes.

4. DISCUSSION

The biophysical profile of RBCs as detected in AFM studies likely contribute to deterioration in hemorheology and hemodynamics, while complicating cardiovascular indices. AEM values representing the mean YM of assessed cellular membranes were increased in RA RBCs, regardless of evident shape changes, indicating a decrease in overall membrane elasticity as AEM values are inversely proportional to degree of elasticity. Decreased RBC membrane elasticity or deformability is indicative of reduced cellular lifespan and could occur via diverse mechanisms associated with oxidative stress and altered membrane composition. Pleiotropic effects of oxidative stress in several inflammatory conditions on several organ-systems triggering cellular apoptosis in RBCs have been described extensively (32-35). Inflammatory immune responses trigger eryptotic pathology via cyclin dependent kinase CDK4 and Gαi2 signalling, leading to ceramide generation and dysregulated cellular calcium influx via cation channels (34-

37). These ultimately activate scramblase which induces phosphatidylserine transfer to the external leaflet (38, 39). Membrane blebbing, morphopathology and microparticle formation follows, conferring a procoagulatory phenotype to affected RBCs (40, 41). RBC-originating microparticles are also reported to have procoagulatory and immunomodulatory activities (42-44). Images from our SEM studies provide evidence that RBC-derived microparticles can remain membrane bound (see figure 7C), conceivably justifying the cell's conferred prothrombotic capacity. Described eryptotic mechanisms may contribute to depletion of circulating RBCs leading to anaemia in arteritis (45). Evidence of contributions from dormant bacteria resuscitated via iron dysregulation, and changes to pathways regulating vitamin D metabolism to these eryptotic changes have been well described (46-49). In aging RBCs, membrane vesiculation occurs through a band-3 centered mechanism, (50) and reduction of membrane elasticity via this mechanism parallels with clinical models of aging RBCs in other morbidities (51). Tyrosine phosphorylation of a cytoplasmic domain within band-3 has been found to cause a disengagement of this glycoprotein from spectrin, leading to its release in microvesicles (52). ATP depletion leading to reduced phosphorylation of spectrin has also been found to result in increased membrane rigidity (53). Increase in plasma cholesterol parameters, membrane signalling that trigger Ca^{2+} influx or downregulate signalling via adenylyl cyclase, cyclic AMP, protein kinase A pathways have also been reported to result in stiffer RBC membranes (54, 55). As 77% of patients in this cohort were diagnosed with lipid imbalance, high cholesterol levels, or related cardiovascular imbalances, this may have contributed to reduced elasticity of their RBCs.

Poikilocytes in RA subjects observed via imaging studies appear to follow a trend characteristic of pathologic or therapeutic influences, such as knizocytes corresponding frequently with NSAID use and stomatocytes frequently detected in patients with cardiovascular complications. However, other factors described in literature may be contributing to the formation of these poikilocytes in RA subjects. It was evident from AFM outcome that there was a mean decrease in membrane elasticity, regardless of presence or quantity of visible morphological lesions as detected via SEM. It is possible that apoptosis is a gradual process, reflecting in covertly abnormal membrane pathology (and correspondingly subtle changes to RBC indices) while much more extensive cellular changes result in visible eryptotic morphology, culminating in significantly altered hemorheology. The appraisal of outcomes from other studies and ours supports this. Increase in hemorheological parameters like blood and plasma viscosity and filterability have long been demonstrated in RA as such (56).

Two poikilocytes frequently identified via imaging studies were knizocytes and stomatocytes. Knizocytes could be induced by the interaction of non-steroidal anti-inflammatory drugs on acyl chains of the phospholipid bilayer (57). It was also identified at high frequency in a case-study of an individual who overdosed on paracetamol (58). This interaction may explain the finding considering that over 70% of the patients in this cohort were on NSAIDs. The stomatocyte transformation has previously been associated with free radical damage in certain patients with chronic fatigue syndrome (5). Chemical, biological, or physical agents capable of reducing the composition of outer membrane leaflet relative to inner have been theorized to induce a stomatocyte transformation and progressively lead to spherocyte formation

and these influences are quite pronounced in this RA cohort (59). Altered membrane phospholipid or cholesterol induced by lysophospholipids, fatty acids or diverse chemical agents have been reported to lead to the formation of echinocytes (reversible) or acanthocytes (irreversible) (24, 59). Irregularly contracted cells, thought to be a nonspecific finding in several inflammatory conditions, reflect instability of cellular haemoglobin brought on by oxidative stress (60, 61). Dacryocytes or teardrop cells were recently identified as hallmark features in autoimmune and microangiopathic haemolytic anemia (62). Thus, this finding may occur in RA RBCs in this study due to autoantibody activities on the membrane. RBCs with knots, dubbed knot-cells, have been identified in other inflammatory conditions, and confirm destabilization of the protein scaffold, which should maintain membrane integrity (24). High plasma levels of low-density lipoproteins or the presence of anemias can also result in the formation of spherocytes (61) and this was supported in the finding of spherocytes in the patient with anemia. Leptocytes, previously identified in RA have also been associated with oxidative stress in RBCs (5). Anemia caused by chronic diseases, which RA is categorized as, can also be a reason for the occurrence of elliptocytes also known as ovalocytes or pencil cells (61, 63). Dysregulation of erythropoiesis has also been thought to result in findings of dual combinations of poikilocytes such as with the knizodacryocyte (61). Several of these morphological transformations may reflect a compromise in configuration of the RBC's underlying skeletal membrane network, a phenomenon which is confirmed in CM findings.

Lai and coworkers established an association between disengagement in positioning of the triangular spectrin-complexed cytoskeletal network and membrane stiffening

supportive of findings from malaria-infected RBCs (64). Disengagement of spectrin could be occurring concurrently with the loss of band 3 proteins within membrane vesicles, as described earlier, resulting in increased tension at the extracellular surface. Besides, upon holistic examination, the layout of protein epitopes within the membrane distinguished a skeletal framework in RA RBCs that were less circular and non-supportive of a discoid membrane visible in the 2-dimensional outlines forming cellular cross-sections. A change in distribution patterns of the band 3 network with increased axial ratio, reduced circularity, roundness, and solidity are evidence suggesting loss of this protein from RA RBC membranes. These changes reflect reduced surface area on the membrane outer leaflet, which would support the stomatocytes configuration, as frequently detected. Loss of band 3 within RBC-originating membrane vesicles could be a mechanism through which the RBC contributes to dysfunctional hemorheology and cardiovascular pathophysiology in RA.

In recent reviews, we described potential mechanisms through which pathological changes to cellular structure can not only reflect inflammatory activity, but also influence disease pathophysiology (24, 43). In one study, a negative correlation was detected between levels of nitric oxide efflux from RBCs and carotid intima thickness (65). In another, altered microvascular function and reduced vasodilator capacity was detected in the microcirculation of patients with chronic systemic inflammatory arthritis (66). Dysfunction in the RBC's regulatory capacity on cerebral vasculature and microcirculation contribute to cardiovascular risk. Consistent with findings from our study, these provide evidence of the contribution of oxidative morphological lesions in erythrocytes to atherosclerotic risk in RA. There is also evidence from

literature that the deformability index contributes to altered hemorheology and hemodynamics, which may influence the risk for the occurrence of cardiovascular complications(18). Erythrocyte morphopathology, as demonstrated in this study, with accompanying elevation in circulating plasma proteins like fibrinogen compound atherosclerotic and cardiovascular risk. In addition, inflammation-triggered bioactive elements such as microparticles, activated platelets, and immune complexes within plasma, are likely to crowd RA vasculature, altering blood viscosity and shear flow parameters. Optimal clearance of affected erythrocytes with stiffer membranes with their congruent microparticles from circulation may also be impeded during transit through splenic sinusoids. This is likely to further aggravate the immune response which is already compromised in these individuals.

5. CONCLUSIONS AND OUTLOOK

This study provides evidence that suggests RBC membrane pathomorphology is an ongoing phenomenon in this RA cohort and this may cause a deterioration in the rheological properties of blood while exacerbating cardiovascular workload. Lipid imbalances, drug use, and degree of oxidative or inflammatory damage generated locally or systemically could all contribute to pathological biophysical changes in RBCs of subjects affected by RA. Findings provide an incentive to monitor RBC integrity in RA sufferers besides serological and clinical factors currently employed.

Prospective research endeavours include investigating specific correlations between changes to biophysical characteristics of blood cells and measures of disease activity markers, duration, blood cytokines, comorbid events, and other clinical indices.

6. List of Abbreviations

ACR – American College of Rheumatology

AEM – Apparent Elastic Modulus

AFM – Atomic force microscopy

ATP – Adenosine triphosphate

Ca^{2+} - Calcium

CM - Confocal microscopy

CV - Cardiovascular

DAI – Disease activity index

HMDS - Hexamethyldisilazane

RA - Rheumatoid arthritis

RBC - Red blood cell

RDW - Red blood cell distribution width

SEM - Scanning electron microscopy

PBS - Sodium phosphate buffer

LM - Light microscopy

NSAID – Non-steroidal anti-inflammatory drug

QNM - Quantitative Nanomechanical Mapping

YM – Young's modulus

7. Conflict of interest declaration

With respect to this study and publication of its findings, the authors have no competing interests to declare.

8. References

1. Halverson PB. Extraarticular manifestations of rheumatoid arthritis. Orthopaedic nursing. 1995;14(4):47-50.
2. Bester J, Pretorius E. Effects of IL-1β, IL-6 and IL-8 on erythrocytes, platelets and clot viscoelasticity. Scientific reports. 2016;6.
3. Cimen MY, Cimen OB, Kaçmaz M, Oztürk HS, Yorgancioğlu R, Durak I. Oxidant/antioxidant status of the erythrocytes from patients with rheumatoid arthritis. Clinical rheumatology. 2000;19(4):275-7.
4. Richards RS, Roberts TK, Mathers D, Dunstan RH, McGregor NR, Butt HL. Investigation of erythrocyte oxidative damage in rheumatoid arthritis and chronic fatigue syndrome. Journal of chronic fatigue syndrome. 2000;6(1):37-46.
5. Richards RS, Roberts TK, Mathers D, Dunstan RH, McGregor NR, Butt HL. Erythrocyte morphology in rheumatoid arthritis and chronic fatigue syndrome. Journal of chronic fatigue syndrome. 2000;6(1):23-35.
6. Woong SL, Think-You K. Relation between red blood cell distribution width and inflammatory biomarkers in rheumatoid arthritis. Archives of pathology & laboratory medicine 134. 2010:505-6.
7. Sprague RS, Ellsworth ML, Stephenson AH, Lonigro AJ. Participation of cAMP in a signal-transduction pathway relating erythrocyte deformation to ATP release. American journal of physiology - cell physiology. 2001;281(4):C1158-C64.
8. Staroń A, Mąkosa G, Koter-Michalak M. Oxidative stress in erythrocytes from patients with rheumatoid arthritis. Rheumatology international. 2012;32(2):331-4.
9. Dupire J, Socol M, Viallat A. Full dynamics of a red blood cell in shear flow. Proceedings of the national academy of sciences. 2012;109(51):20808-13.
10. Peters LL, Shivdasani RA, Liu S-C, Hanspal M, John KM, Gonzalez JM, et al. Anion exchanger 1 (band 3) is required to prevent erythrocyte membrane surface loss but not to form the membrane skeleton. Cell. 1996;86(6):917-27.
11. Rybicki AC, Heath R, Wolf JL, Lubin B, Schwartz RS. Deficiency of protein 4.2 in erythrocytes from a patient with a Coombs negative hemolytic anemia. Evidence for a role of protein 4.2 in stabilizing ankyrin on the membrane. Journal of Clinical Investigation. 1988;81(3):893-901.
12. Lu A, Zha Q, editors. Correlations among cartilage erosion, IgA level, red blood cell and platelet counts in 436 rheumatoid arthritis patients with path analysis. 2009 3rd international conference on bioinformatics and biomedical engineering; 2009; Beijing: ICBBE.
13. Dixey J, Solymossy C, Young A. Is it possible to predict radiological damage in early rheumatoid arthritis (RA)? A report on the occurrence, progression, and prognostic factors of radiological erosions over the first 3 years in 866 patients from the early RA Study (ERAS). Journal of rheumatology Supplement. 2004;69:48-54.
14. Gudmundsson M, Bjelle A. Viscosity of plasma and blood in rheumatoid arthritis. Rheumatology. 1993;32(9):774-9.
15. Yildirim K, Karatay S, Melikoglu MA, Gureser G, Ugur M, Senel K. Associations between acute phase reactant levels and disease activity score (DAS28) in patients with rheumatoid arthritis. Annals of clinical & laboratory science. 2004;34(4):423-6.
16. (NCCDPHP) NCfCDPaHP. Arthritis in America. In: prevention Cfdca, editor. Atlanta, Georgia 30329-4027 USA: Office of the associate director for communications; 2017.
17. Agca R, Heslinga SC, Rollefstad S, Heslinga M, McInnes IB, Peters MJL, et al. Eular recommendations for cardiovascular disease risk management in patients with rheumatoid arthritis and other forms of inflammatory joint disorders: 2015/2016 update. Annals of the rheumatic diseases. 2016;76(1):17-28.
18. Cicco G, Pirrelli A. Red blood cell (RBC) deformability, RBC aggregability and tissue oxygenation in hypertension. Clinical hemorheology and microcirculation. 1999;21(3-4):169-77.

19. Patel KV, Mohanty JG, Kanapuru B, Hesdorffer C, Ershler WB, Rifkind JM. Association of the red cell distribution width with red blood cell deformability. Advances in experimental medicine and biology. 2013;765:211-6.
20. Zhou Y, Zhang Q, Yan L, Li Y, Hua L. Association between red cell distribution width and myocardial infarction in rheumatoid arthritis. Clinical chemistry and laboratory medicine. 2015;53(7):e153-e5.
21. Harrison ML, Rathinavelu P, Arese P, Geahlen RL, Low PS. Role of band 3 tyrosine phosphorylation in the regulation of erythrocyte glycolysis. Journal of biological chemistry. 1991;266(7):4106-11.
22. Van Kim CL, Colin Y, Cartron J-P. Rh proteins: key structural and functional components of the red cell membrane. Blood reviews. 2006;20(2):93-110.
23. Mouro-Chanteloup I, Delaunay J, Gane P, Nicolas V, Johansen M, Brown EJ, et al. Evidence that the red cell skeleton protein 4.2 interacts with the rh membrane complex member cd47. Blood. 2003;101(1):338-44.
24. Pretorius E, Olumuyiwa-Akeredolu O-O, Mbotwe S, Bester J. Erythrocytes and their role as health indicator: using structure in a patient-orientated precision medicine approach. Blood reviews. 2016;30(4):263-74.
25. Cazzola R, Rondanelli M, Russo-Volpe S, Ferrari E, Cestaro B. Decreased membrane fluidity and altered susceptibility to peroxidation and lipid composition in overweight and obese female erythrocytes. Journal of lipid research. 2004;45(10):1846-51.
26. Arbustini E. Total erythrocyte membrane cholesterol. Journal of the american college of cardiology. 2007;49(21):2090.
27. Smolen JS, Aletaha D, Redlich K. The pathogenesis of rheumatoid arthritis: new insights from old clinical data? Nature reviews rheumatology. 2012:235-43.
28. Derjaguin BV, Muller VM, Toporov YP. Effect of contact deformations on the adhesion of particles. Journal of colloid and interface science. 1975;53(2):314-26.
29. Foundation TR. R: a language and environment for statistical computing Vienna, Austria: R foundation for statistical computing; 2017 [Available from: https://cran.r-project.org/.
30. Buys AV, Van Rooy M-J, Soma P, Van Papendorp D, Lipinski B, Pretorius E. Changes in red blood cell membrane structure in type 2 diabetes: a scanning electron and atomic force microscopy study. Cardiovascular diabetology2013.
31. Papadopulos F, Spinelli M, Valente S, Foroni L, Orrico C, Alviano F, et al. Common tasks in microscopic and ultrastructural image analysis using imagej. Ultrastructural pathology. 2007;31(6):401-7.
32. Lupescu A, Bissinger R, Goebel T, Salker MS, Alzoubi K, Liu G, et al. Enhanced suicidal erythrocyte death contributing to anemia in the elderly. Cellular physiology and biochemistry. 2015;36(2):773-83.
33. Pretorius E, Swanepoel AC, Buys AV, Vermeulen N, Duim W, Kell DB. Eryptosis as a marker of Parkinson's disease. Aging (Albany NY). 2014;6(10):788-819.
34. Pretorius E, du Plooy JN, Bester J. A comprehensive review on eryptosis. Cellular physiology and biochemistry. 2016;39(5):1977-2000.
35. Bissinger R, Schumacher C, Qadri SM, Honisch S, Malik A, Gotz F, et al. Enhanced eryptosis contributes to anemia in lung cancer patients. Oncotarget. 2016;7(12):14002-14.
36. Lang E, Zelenak C, Eberhard M, Bissinger R, Rotte A, Ghashghaeinia M, et al. Impact of cyclin-dependent kinase CDK4 inhibition on eryptosis. Cellular physiology and biochemistry. 2015;37(3):1178-86.
37. Bissinger R, Lang E, Ghashghaeinia M, Singh Y, Zelenak C, Fehrenbacher B, et al. Blunted apoptosis of erythrocytes in mice deficient in the heterotrimeric G-protein subunit Gαi2. Scientific reports. 2016;6:30925.
38. Qadri SM, Donkor DA, Bhakta V, Eltringham-Smith LJ, Dwivedi DJ, Moore JC, et al. Phosphatidylserine externalization and procoagulant activation of erythrocytes induced by

Pseudomonas aeruginosa virulence factor pyocyanin. Journal of cellular and molecular medicine. 2016;20(4):710-20.
39. Lang E, Qadri SM, Lang F. Killing me softly - suicidal erythrocyte death. International journal of biochemistry & cell biology. 2012;44(8):1236-43.
40. Lang E, Bissinger R, Fajol A, Salker MS, Singh Y, Zelenak C, et al. Accelerated apoptotic death and in vivo turnover of erythrocytes in mice lacking functional mitogen- and stress-activated kinase MSK1/2. Scientific reports. 2015;5:17316.
41. Qadri SM, Bissinger R, Solh Z, Oldenborg PA. Eryptosis in health and disease: a paradigm shift towards understanding the (patho)physiological implications of programmed cell death of erythrocytes. Blood reviews. 2017.
42. Berckmans RJ, Nieuwland R, Tak PP, Böing AN, Romijn FPHTM, Kraan MC, et al. Cell‐derived microparticles in synovial fluid from inflamed arthritic joints support coagulation exclusively via a factor VII–dependent mechanism. Arthritis & rheumatism. 2002;46(11):2857-66.
43. Olumuyiwa-Akeredolu OO, Pretorius E. Platelet and red blood cell interactions and their role in rheumatoid arthritis. Rheumatology international. 2015;35(12):1955-64.
44. Distler JHW, Pisetsky DS, Huber LC, Kalden JR, Gay S, Distler O. Microparticles as regulators of inflammation: novel players of cellular crosstalk in the rheumatic diseases. Arthritis & rheumatism. 2005;52(11):3337-48.
45. Bissinger R, Kempe-Teufel DS, Honisch S, Qadri SM, Randrianarisoa E, Haring HU, et al. Stimulated suicidal erythrocyte death in arteritis. Cellular physiology and biochemistry. 2016;39(3):1068-77.
46. Lang E, Jilani K, Bissinger R, Rexhepaj R, Zelenak C, Lupescu A, et al. Vitamin D-rich diet in mice modulates erythrocyte survival. Kidney and blood pressure research. 2015;40(4):403-12.
47. Pretorius E, Bester J, Kell DB. A bacterial component to alzheimer's-type dementia seen via a systems biology approach that links iron dysregulation and inflammagen shedding to disease. Journal of alzheimers disease. 2016;53(4):1237-56.
48. Pretorius E, Akeredolu O-O, Soma P, Kell DB. Major involvement of bacterial components in rheumatoid arthritis and its accompanying oxidative stress, systemic inflammation and hypercoagulability. Experimental biology and medicine. 2017;242(4):355-73.
49. Baker JF, Ghio AJ. Iron homoeostasis in rheumatic disease. Rheumatology. 2009;48(11):1339-44.
50. Bosman GJCGM, Lasonder E, Groenen-Döpp YAM, Willekens FLA, Werre JM. The proteome of erythrocyte-derived microparticles from plasma: new clues for erythrocyte aging and vesiculation. Journal of proteomics. 2012;76(0):203-10.
51. Pavlova TV, Prashchayeu KI, Pozdnyakova NM, Legkii VN, Bashuk VV, Nesterov AV, et al. Morphofunctional features of erythrocytes as targets of early aging. Advances in gerontology. 2014;4(1):51-4.
52. Puchulu-Campanella E, Turrini FM, Li Y-H, Low PS. Global transformation of erythrocyte properties via engagement of an SH2-like sequence in band 3. Proceedings of the national academy of sciences. 2016;113(48):13732-7.
53. Picas L, Rico F, Deforet M, Scheuring S. Structural and mechanical heterogeneity of the erythrocyte membrane reveals hallmarks of membrane stability. ACS nano. 2013;7(2):1054-63.
54. Babu N. Influence of hypercholesterolemia on deformability and shape parameters of erythrocytes in hyperglycemic subjects. Clinical hemorheology and microcirculation. 2009;41(3):169-77.
55. Muravyov AV, Tikhomirova IA. Role molecular signaling pathways in changes of red blood cell deformability. Clinical hemorheology and microcirculation. 2013;53(1):45-59.
56. Ernst E, Thies W, Matrai A, Seichert N, Schöps P, Magyarosy I, et al. Hemorheological abnormalities in rheumatoid arthritis. Clinical hemorheology and microcirculation. 1987;7(4):591-8.

57. Suwalsky M, Manrique M, Villena F, Sotomayor CP. Structural effects in vitro of the anti-inflammatory drug diclofenac on human erythrocytes and molecular models of cell membranes. Biophysical chemistry. 2009;141(1):34-40.
58. Lesesve JF, Garçon L, Lecompte T. Finding knizocytes in a peripheral blood smear. American journal of hematology. 2012;87(1):105-6.
59. Lim HWG, Wortis M, Mukhopadhyay R. Stomatocyte–discocyte–echinocyte sequence of the human red blood cell: Evidence for the bilayer– couple hypothesis from membrane mechanics. Proceedings of the national academy of sciences. 2002;99(26):16766-9.
60. Bain BJ. Diagnosis from the blood smear. New england journal of medicine. 2005;353(5):498-507.
61. Ford J. Red blood cell morphology. International journal of laboratory hematology. 2013;35(3):351-7.
62. Robier C, Klescher D, Reicht G, Amouzadeh-Ghadikolai O, Quehenberger F, Neubauer M. Dacryocytes are a common morphologic feature of autoimmune and microangiopathic haemolytic anaemia. Clinical chemistry and laboratory medicine. 2015;53(7):1073-6.
63. Harrington AM, Ward PC, Kroft SH. Iron deficiency anemia, beta-thalassemia minor, and anemia of chronic disease: a morphologic reappraisal. American journal of clinical pathology. 2008;129(3):466-71.
64. Lai L, Xu X, Lim CT, Cao J. Stiffening of red blood cells induced by cytoskeleton disorders: a joint theory-experiment study. Biophysical journal. 2015;109(11):2287-94.
65. Saldanha C. Physiological role of erythrocyte nitric oxide. Clinical hemorheology and microcirculation. 2016;64(4):517-20.
66. Klimek E, Sulicka J, Gryglewska B, Skalska A, Kwaśny-Krochin B, Korkosz M, et al. Alterations in skin microvascular function in patients with rheumatoid arthritis and ankylosing spondylitis. Clinical hemorheology and microcirculation. 2017;65(1):77-91.